Materials Research. 2017; 20(3): 712-717
DOI: http://dx.doi.org/10.1590/1980-5373-MR-2016-0786

Thickness Dependent Structural and Electrical Properties of Magnetron Sputtered Nanostructured CrN Thin Films

Harish Sharma Akkera[b], Nallabala Nanda Kumar Reddy[b], Musalikunta Chandra Sekhar[a]*

[a] Department of Electronic Engineering, Yeungnam University, 280 Daehak-ro Gyeongsan-si Gyeongsangbuk-do, 3854, Republic of Korea
[b] Department of Physics, Madanapalle Institute of Technology & Science, Madanaplle, Andhra Pradesh-517325, India

Received: October 21, 2016; Revised: February 15, 2017; Accepted: March 09, 2017

In the present work, we have investigated the structural and electrical properties of CrN thin films for a thickness *t* in the 30-220 nm range, grown on Si (100) substrates. The CrN/Si (100) films exhibits a structural transition from hexagonal phase (β-Cr_2N) to cubic phase (CrN) with the increasing in film thickness, the change in structural transition is attributed to the decrease of film-substrate interfacial strain. From electrical resistivity measurements, the thickness of 150 nm CrN/Si (100) film shown the metal-semiconductor phase transition at around 250 K with energy band gap (E_g) 81 meV in semiconducting region, whereas the thickness of 30, 110 and 220 nm CrN/Si(100) films were shown only semiconducting behaviour for whole temperature range of 50-400 K. On the other hand, a clear grain size was increased in CrN/Si films with increasing thickness and its influence on transport properties was also seen. The possibility of phase transition and occurrence of semiconducting behaviour in the CrN films were analysed.

Keywords: *Magnetron sputtering, CrN thin films, Metal-Semiconducting phase transition*

1. Introduction

Over the past decades, CrN has received a great technological attention due to its remarkable mechanical properties such as high hardness, high wear resistance, and high temperature oxidation resistance[1-3]. Besides the technological importance, CrN also shows very interesting novel properties like magnetic, optical, and electronic properties. It is well known that bulk CrN is paramagnetic behaviour (PM) at room temperature with a B1 NaCl crystal structure. At the Neel temperature in a range of 273-283 K it undergoes a first order phase transition to antiferromagnetic (AFM) with an orthorhombic *Pnma* Crystal structure[4,5]. However, many authors studied the structural, electrical, mechanical and magnetic properties of CrN thin films grown on different substrates, such as Si (100), MgO (001) and Al_2O_3 (0001) etc.[6-11]. Recently, Ney et al.[12] reported that the CrN thin films deposited on MgO (001) substrate and Al_2O_3 (0001) substrate showed the paramagnetic behaviour at low temperature and ferromagnetic behaviour above room temperature, respectively. Filippetti et al.[13] concluded that CrN was a metal in its PM state but a weak metal in the antiferromagnetic state. Constantin et al.[14] observed that electronic, magnetic and structural phase transitions might be correlated in CrN/MgO film deposited by molecular-beam epitaxy method. Some experimental studies revealed different results on the electron transport properties of CrN material. Therefore, it is still open issue in this material how the structural and electronic phase transitions are correlated[15]. In this study, CrN thin films grown on Si (100) substrates at different thickness ranges, 30-220 nm, by reactive dc magnetron sputtering and systematically examined the structural and electrical properties.

2. Experimental Details

The different thicknesses CrN thin films were grown onto Si (100) substrates using dc reactive magnetron sputtering at 350°C temperature. High purity (99.99%) Cr metal target of 50 mm diameter and 3 mm thickness was used. Before sputtering deposition, the chamber was evacuated to a base pressure of the order of 2×10^{-6}torr and no post annealing was performed after deposition. Working pressure was maintained at a constant value of 10 m Torr. The target and substrate distance was kept constant approximately 5 cm. The deposition was carried out for 5, 10, 15 and 20 min to get the different thicknesses (30, 90, 150, 220 nm) and power was kept constant at 90 W for all depositions. The chamber environment was 70%Ar+ 30%N_2 during deposition. The crystallographic orientations of the deposited films were studied using a Bruker advanced diffractrometer of Cu Kα (1.54Å) radiations in θ–2θ geometry at a scan speed of 1°/min. The deposited films were subjected to morphological characterization using Zeiss Evo18 Scanning electron microscope (SEM) and atomic force microscopy (AFM). The resistivity verses temperatures (ρ-T) measurements were performed by four-probe resistivity method using a cryohead with helium compressor interfaced with Keithley instruments over temperature range from 50 K to 400 K.

* e-mail: chandu.phys@gmail.com

3. Results and Discussion

Figure 1 shows the XRD patterns of CrN films with different thicknesses grown on Si (100) substrates. The CrN/Si (100) films with thicknesses t = 30 nm was found to be hexagonal (β- Cr_2N) crystal structure with preferred (002) orientation along with small orientation peaks (200) and (311), and further increasing thickness (t =150 and 220nm) the films were exhibited structural phase transition from hexagonal β-Cr_2N with (002) orientation to (111) orientation of cubic CrN. The film with an intermediate thickness of 90 nm was found to have mixed phase of hexagonal β-Cr_2N (002) and cubic CrN phase with fundamental peak (111) and small intensity of (200) and (311) peaks were observed. Many authors were reported in the literature, the CrN films exhibits structural phase transition from NaCl cubic crystal structure at room temperature to orthorhombic structure at Neel temperature[16]. In this present study, the CrN/Si films exhibited structural transition due to the variation of thickness. Nevertheless, we have noticed the mixed CrN phase for the 90 nm film due to structural transition from the lower thickness of hexagonal β-Cr_2N phase to higher thickness of cubic CrN phase. This structural transition could be due to the lattice misfit of CrN phase w.r.t to substrate. In order to investigate the micro structural properties, we studied the scanning electron microscope (SEM) and atomic force microscopy (AFM) analysis for all deposited CrN/Si (100) films. Figure 2(a)-(d) and Figure 3(a)-(d) depicts the scanning electron microscope (SEM) and atomic force microscope (AFM) microstructures of various thicknesses (t = 30, 90, 150 and 220 nm) of CrN/Si (100) films, respectively. The SEM and AFM images show that the CrN thickness effectively changes the microstructure of the films. All deposited films were homogeneous and crack-free. Both SEM and AFM microstructures replicate an increase in grain size with increasing of CrN thickness and all the films are spherical grains in nature. The values of average grain size (for both SEM and AFM) and root mean square (RMS) surface roughness were given in Table 1. The grain size and RMS roughness of the films were observed to increase with the increasing CrN thickness. Figure 4 (a) shows electrical resistivity as a function of temperature ρ (T) measured between 50 K to 400 K of all CrN/Si (100) films with different thicknesses. Thickness of 150 nm CrN/Si film was polycrystalline cubic structure in nature conformed from XRD results. In the ρ (T) curve, the t =90 nm CrN/Si film resistivity (ρ) slightly decreasing with increasing T between 50 and 250 K, showing semiconducting behaviour with $d\rho/dT < 0$. At 250 K, ρ begins to increase sharply and reaches 284 K, it indicates the metallic behvior with $d\rho/dT > 0$. Further increasing the

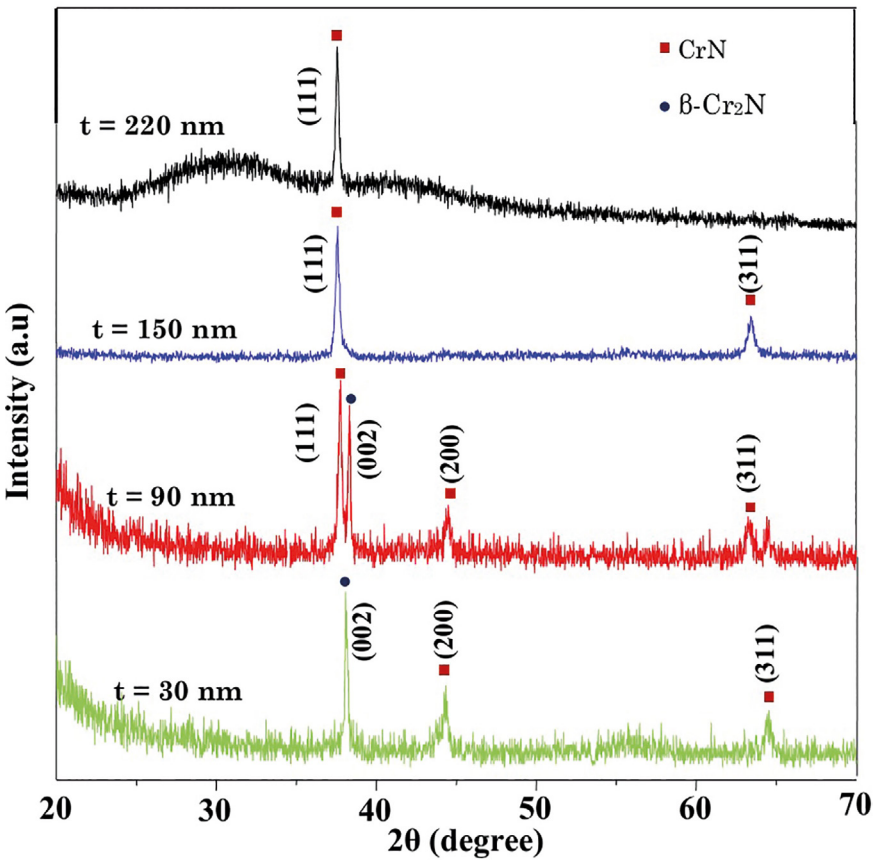

Figure 1. XRD pattern of different thicknesses of CrN/Si (100) films.

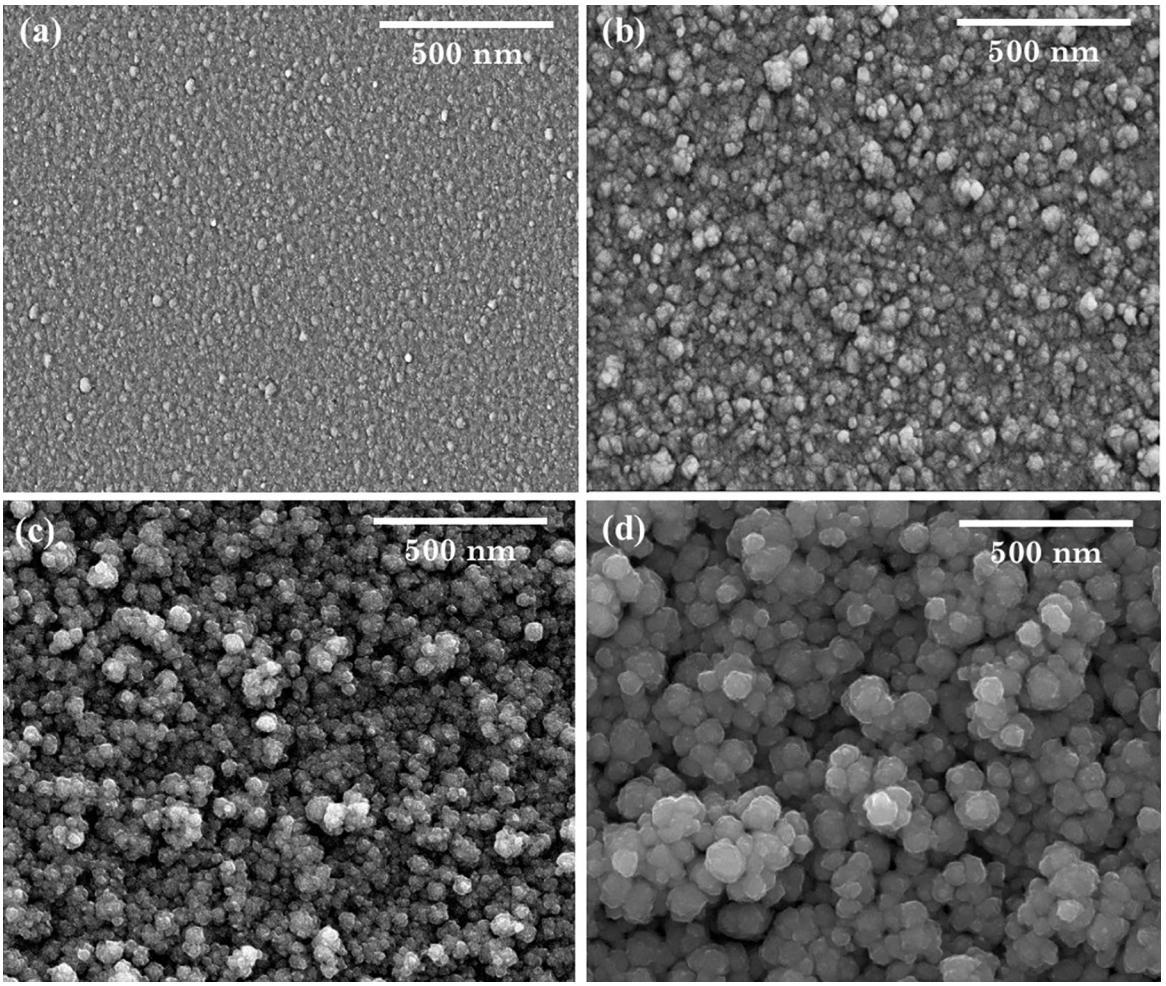

Figure 2. SEM images of (a) t = 30 nm, (b) t = 90 nm, (c) t = 150 nm and (d) t = 220 nm CrN/Si (100) films.

temperature from 284 K to 400 K, the ρ decreasing sharply showed the semiconducting behaviour, this could be attributed to the presence of a band gap or carrier localization due to grain boundaries or N-vacancies[17,18]. The room temperature resistivity is 36.6 Ω-cm, this is within the wide range of previously reported values, 3×10^{-4} to 600 Ω-cm, obtained from polycrystalline CrN thin films[19]. The resistivity shows the discontinuity at around 250-284 K (marked in curve), as shown in Figure 4(b), which is associated with a structural phase transition. This discontinuity could be occurred due to the grain boundary changes in the film and as well as changing in the shape and volume of the unit cell during phase transition[20]. Most polycrystalline CrN films exhibits the phase transitions due to distort the individual grains in different directions and the associated volume reduction would provide sufficient space within the microstructure for grain boundary slide. To study the electrical transport mechanism of this film, we have fitted the curve above the Neel temperature (T_N) of CrN in the semiconducting (284-400 K) region, as shown in Figure 5.

By using an activation law

$$\rho(T) = \rho_0 * \exp(E_g/2KT) \quad (1)$$

we have calculated the slope of the curve equal to $E_g/2K$ and corresponding E_g value 80 meV with ρ_0=4.59 × 10^{-3} Ω cm, the room temperature resistivity $\rho_{300\,K}$ = 36.6 Ω-cm. The E_g value is consistent with these previously reported values and range from 48 to 81 meV[14].

Further, the thickness of t= 30, 1 50 and 220 nm CrN films deposited on Si (100) substrates shows the resistivity decreases monotonically with increasing temperature range 50- 400 K, and shows no discontinuity at around 280 K, suggesting no phase transition. This is in contrast to some earlier reported authors[4,21]. Here, XRD results shows that t = 30 nm CrN film is a hexagonal crystal structure and not shown any structural phase transition in ρ (T) curve, this could be due to the lack of appropriate N-vacancy concentration in this thickness for the phase transition. When thickness reaches t = 150 nm, cubic phase, shown

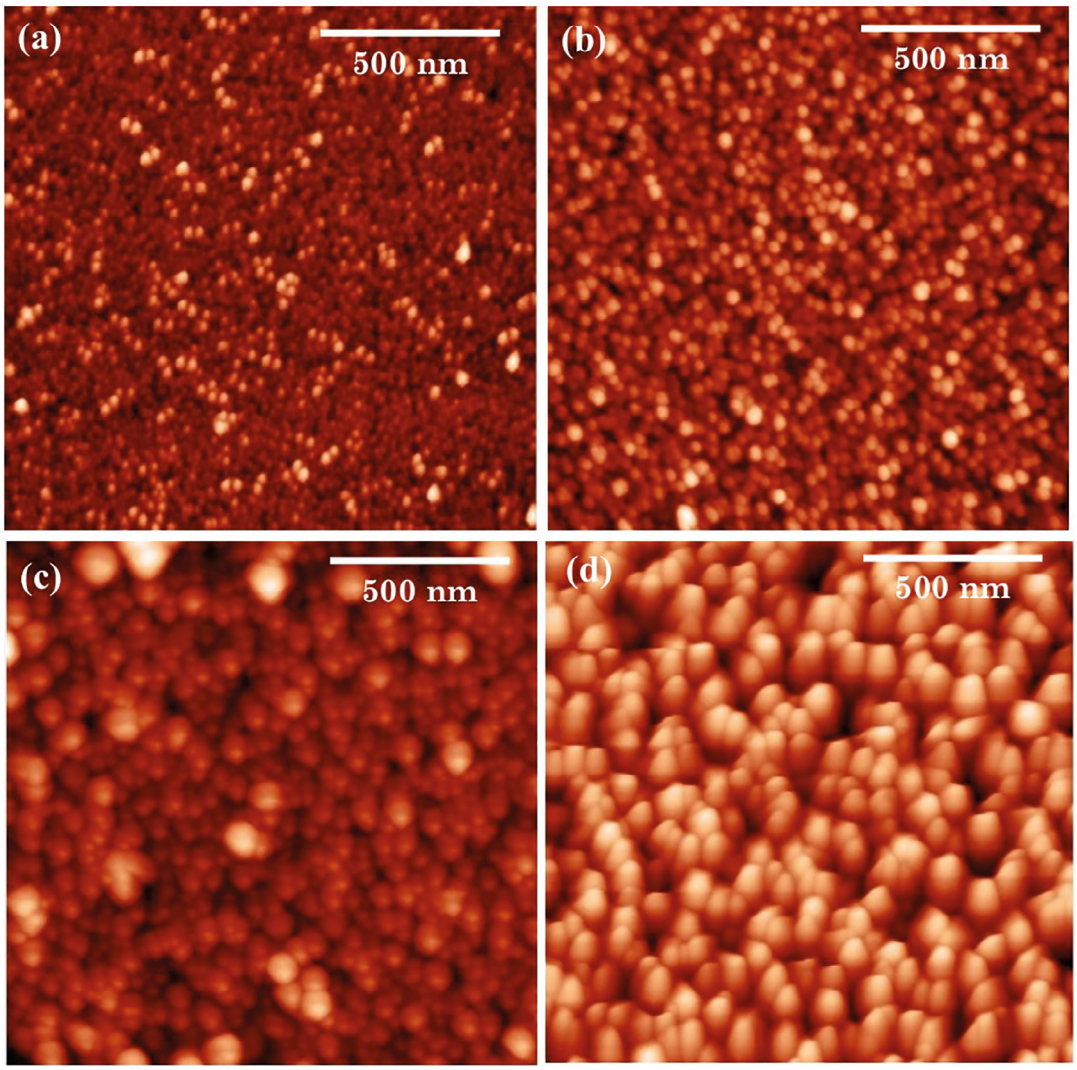

Figure 3. AFM microstructures of (a) t = 30 nm, (b) t = 90 nm, (c) t = 150 nm and (d) t = 220 nm CrN/Si (100) films.

Table 1. Various parameters of different thicknesses of CrN/Si(100) films

Thickness (t) of CrN/Si(100) film	Crystallographic Phase	Average grain size (nm)		RMS roughness (nm)	ρ300 (Ω-cm)
		SEM	AFM		
30	Hexagonal β-Cr2N	62±3	68±2	2.3	25.6
90	Mixed (Hexagonal and cubic)	79±4	88±3	5.6	36.6
150	Cubic CrN	105±4	111±2	7.2	42.2
220	Cubic CrN	138±3	143±2	7.6	63.9

only semiconducting behaviour entire temperature range. The resistivity of the film fabricated with thickness t = 220 nm film also exhibiting semiconducting behaviour. Among all the thicknesses, t = 90 nm CrN/Si film only shown the phase transition, this thickness is called critical thickness of the CrN film deposited on Si (100) substrate. The structure of t = 220nm CrN/Si film having the perfect lattice with cubic (111) single orientation, due to perfect lattice, makes the transition is very difficult; this could be one of the factor to absence of phase transition[3]. The absolute room temperature resistivity (ρ_{300K}) values were found to be 25.6, 36.6, 42.2 and 63.9 Ω-cm, with increasing thickness t = 30, 90, 150, and 220 nm, respectively. The values were reported in Table 1. Moreover, for the thicknesses t = 30, 150 and 220 nm CrN films resistivity decreases monotonically with increasing temperature and show no first order phase transition. The temperature variations of resistivity are not the simple activation type one. The data are fitted using a Mott variable-

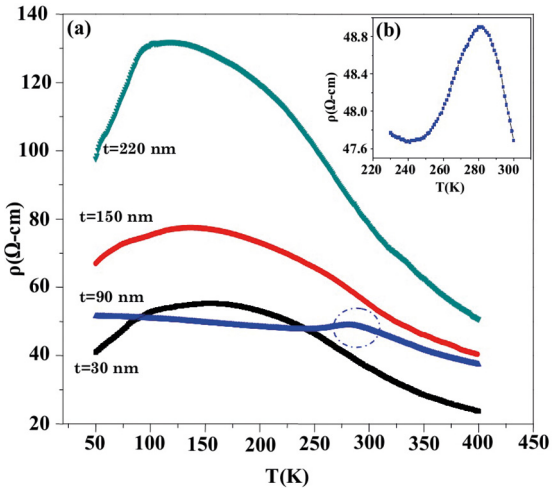

Figure 4. Resistivity versus temperature ρ(T) curves of different thicknesses of CrN/Si (100)films.

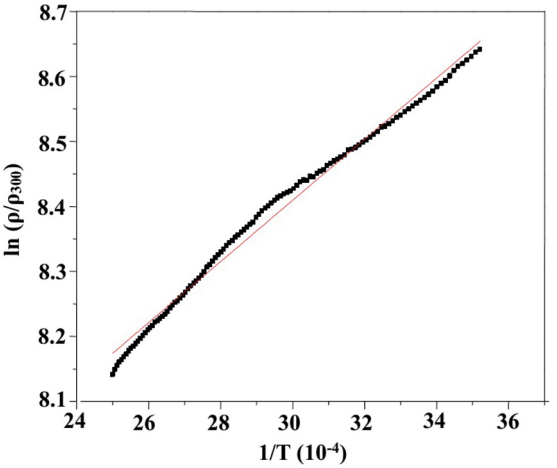

Figure 5. Fitting curve of t = 90 nm CrN/Si (100) in the semiconducting (284-400 K) region.

range hopping (VRH) conduction mechanism with $\rho \alpha T^{-1/4}$ [22,23]. Mott VRH describes well the temperature dependence of ρ for approximately 50-230 K, for all thicknesses t = 30, 150 and 220 nm of CrN films. This suggests a hopping like conduction mechanism is fitted for our semiconducting CrN thin films in the region of 50-230 K. When the film thickness is decreased, the relative impact of the strain generated at the film-substrate interface becomes increasingly important and result in the change of electrical properties of these films. On the other hand, AFM micrographs indicated that the thicker films have larger grain size, the larger grain size results in a lower density of grain boundaries, which behaves as traps for free carriers and barriers for carrier transport in the film[24]. Hence, an increase in grain size can cause a decrease in grain boundary scattering, which leads to decrease in resistivity.

4. Conclusions

In the summery, we have successfully deposited CrN thin films for a thickness *t* in the 30-220 nm range onto Si (100) substrate and investigated the structural and electrical properties. Deposited CrN/Si (100) films have showed structural transition from hexagonal phase (β-Cr_2N) to cubic phase (CrN) with the increasing in film thickness. From ρ (T) measurements, the thickness of 150 nm CrN/Si (100) film shown the metal-semiconductor phase transition at around 250 K with energy band gap (E_g) 81 meV in semiconducting region. Further, AFM microstructures shown CrN/Si films grain size increases with increasing of thickness.

5. References

1. Wiklund U, Bromark M, Larsson M, Hedenqvist P, Hogmark S. Cracking resistance of thin hard coatings estimated by four-point bending. *Surface and Coatings Technology*. 1997;91(1-2):57-63.

2. Nouveau C, Djouadi MA, Banakh O, Sanjinés R, Lévy F. Stress and structure profiles for chromium nitride coatings deposited by r.f. magnetron sputtering. *Thin Solid Films*. 2001;398-399:490-495.

3. Shah HN, Jayaganthan R, Kaur D, Chandra R. Influence of sputtering parameters and nitrogen on the microstructure of chromium nitride thin films deposited on steel substrate by direct-current reactive magnetron sputtering. *Thin Solid Films*. 2010;518(20):5762-5768.

4. Corliss LM, Elliott N, Hastings JM. Antiferromagnetic Structure of CrN. *Physical Review*. 1960;117(4):929.

5. Ibberson RM, Cywinski R. The magnetic and structural transitions in CrN and (CrMo)N. *Physica B: Condensed Matter*. 1992;180-181(Pt 1):329-332.

6. Gall D, Shin CS, Haasch RT, Petrov I, Greene JE. Band gap in epitaxial NaCl-structure CrN (001) layers. *Journal of Applied Physics*. 2002;91(9):5882.

7. Shah HN, Jayaganthan R, Pandey AC. Nanoindentation study of magnetron-sputtered CrN and CrSiN coatings. *Materials &Design*. 2011;32(5):2628-2634.

8. Subramanian B, Prabhakaran K, Jayachandran M. Influence of nitrogen flow rates on materials properties of CrN_x films grown by reactive magnetron sputtering. *Bulletin of Materials Science*. 2012;35(4):505-511.

9. Martinez E, Sanjinés R, Banakh O, Lévy F. Electrical, optical and mechanical properties of sputtered CrN_y and $Cr_{1-x}Si_xN_{1.02}$ thin films. *Thin Solid Films*. 2004;447-448:332-336.

10. Mayrhofer PH, Rovere F, Moser M, Strondl C, Tietema R. Thermally induced transitions of CrN thin films. *ScriptaMaterialia*. 2007;57(3):249-252.

11. Inumaru K, Koyama K, Imo-oka N, Yamanaka S. Controlling the structural transition at the Néel point of CrN epitaxial thin films using epitaxial growth. *Physical Review B*. 2007;75(5):054416.

12. Ney A, Rajaram R, Parkin SSP, Kammermeier T, Dhar S. Magnetic properties of epitaxial CrN films. *Applied Physics Letters*. 2006;89(11):112504.

13. Filippetti A, Pickett WE, Klein BM. Competition between magnetic and structural transitions in CrN. *Physical Review B*. 1999;59(10):7043.

14. Constantin C, Haider MB, Ingram D, Smith AR. Metal/semiconductor phase transition in chromium nitride (001) grown by rf-plasma-assisted molecular-beam epitaxy. *Applied Physics Letters*. 2004;85(26):6371-6373.

15. Zhou Z, Luo S, Wang Y, Ai Z, Liu C, Wang D, et al. Room temperature ferromagnetism and hopping transport in amorphous CrN thin films. *Thin Solid Films*. 2011;519(6):1989-1992.

16. Zhang XY, Chawla JS, Deng RP, Gall D. Epitaxial suppression of the metal-insulator transition in CrN. *Physical Review B*. 2011;84(7):073101.

17. Duan XF, Mi WB, Guo ZB, Bai HL. A comparative study of transport properties in polycrystalline and epitaxial chromium nitride films. *Journal of Applied Physics*. 2013;113(2):023701.

18. Emery C, Chourasia AR, Yashar P. A study of CrN_x thin films by X-ray photoelectron spectroscopy. *Journal of Electron Spectroscopy and Related Phenomena*. 1999;104(1-3):91-97.

19. Mott N. On metal-insulator transitions. *Journal of Solid State Chemistry*. 1990;88(1):5-7.

20. Ruden A, Restrepo-Parra E, Paladines AU, Sequeda F. Corrosion resistance of CrN thin films produced by dc magnetron sputtering. *Applied Surface Science*. 2013;270:150-156.

21. Elangovan T, Kuppusami P, Thirumurugesan R, Ganesan V, Mohandas E, Mangalraj D. Nanostructured CrN thin films prepared by reactive pulsed DC magnetron sputtering. *Materials Scinece and Engineering B*. 2010;167(1):17-25.

22. Mott NF, Davis EA. *Electronic Processes in Non-Crystalline Materials*. 2nd ed. Oxford: Clarendon Press; 1979.

23. Mott NF. *Metal-Insulator Transitions*. 2nd ed. Bristol: Taylor & Francis; 1990.

24. Lin J, Zhang N, Sproul WD, Moore JJ. A comparison of the oxidation behavior of CrN films deposited using continuous dc, pulsed dc and modulated pulsed power magnetron sputtering. *Surface and Coatings Technology*. 2012;206(14):3283-3290.